U.S. DEPARTMENT OF **ENERGY** | Office of Science

FY 2021 Second Quarter Performance Metric: Improve and Validate Earth System Model Simulations of Precipitation Related to Landfalling Hurricanes in the CONUS

April 2021

DISCLAIMER

Contents

Figures

1.0   Product Definition

Extreme precipitation and subsequent severe flooding has been implicated as the primary cause of tropical cyclone (TC)-related fatalities over the past 30 years, as well as the leading cause of infrastructural damage related to these storms (Pielke Jr. et al. 2008). As such, TCs and TC-related flooding are responsible for persistent risks to the U.S. east and Gulf coasts. Investments in model improvement and computation at scale have enabled the Department of Energy (DOE) Energy Exascale Earth System Model (E3SM) to produce one of the most realistic Atlantic TC climatologies among global modeling systems (Balaguru et al. 2020). More specifically, global TC frequency, TC lifetime maximum intensities, and the relative distribution of TCs among the different basins are significantly better simulated at high-resolution compared to low-resolution models commonly used in the Coupled Model Intercomparison Project Phases 5 and 6 (CMIP5/6). However, modeling TC coastal impacts also requires realistic simulations of the distribution and characteristics of landfalling TCs, which are sensitive to the large-scale environment in the North Atlantic basin as well as near the coasts. Furthermore, modeling TC-related precipitation remains an ongoing challenge due to sensitivity of TC rainfall to the simulated TC structure and the physics parameterizations used in the models.

DOE investments in software products such as TempestExtremes (Ullrich and Zarzycki 2017) have allowed tracking and characterization of TCs to become a standard part of the E3SM workflow. Building upon this work, recent efforts have also led to a comprehensive and automated evaluation capability for TCs (Zarzycki et al. 2021, Stansfield et al. 2020), thus enabling developers to quickly identify potential model biases. Further efforts are underway to develop evaluation metrics and diagnostics that evaluate the underlying processes and large-scale environment of TCs, and impacts related to TCs.

In this document, we evaluate the performance of E3SM for modeling landfalling TC precipitation and demonstrate improvement in TC-related precipitation in E3SM at high resolution (28km grid spacing) compared to the standard low resolution (110km grid spacing typical for CMIP models). Our analysis shows that high model resolution enables more accurate simulation of the properties of landfalling storms along the Atlantic and Gulf coasts, particularly with regards to the storm structure. We also demonstrate that, under a variety of salient metrics, E3SM storm structure is particularly realistic, while bias in TC climatology largely comes from subtle biases in the large-scale environment of the atmosphere and ocean, requiring continued efforts in improving the coupled model.

2.0 Product Documentation

The simulations evaluated in this study use E3SM version 1, as described by Caldwell et al. (2019), in its high-resolution (E3SM-HR) and low-resolution (E3SM-LR) configurations. The model is a fully coupled atmosphere-ocean global climate model (GCM), developed to support DOE's energy mission (Leung et al. 2020). The atmospheric model is described in Rasch et al. (2019). It consists of a spectral-element dynamical core with 72 vertical levels (Dennis et al. 2012) and parameterized physics processes including deep convection (Neale et al. 2008, Richter and Rasch 2008, Zhang and McFarlane 1995); macrophysics, turbulence, and shallow convection (Golaz et al. 2002, Larson 2017, Larson and Golaz 2005); microphysics (Gettelman and Morrison 2015, Gettelman et al. 2015); aerosol treatment (Liu et al. 2016); and radiative transfer (Iacono et al. 2008, Mlawer et al. 1997). The ocean and sea ice

components employ the Model for Prediction Across Scales (Petersen et al. 2019, Ringler et al. 2013). A mesoscale eddy parameterization (Gent and McWilliams 1990) is used only for the E3SM-LR simulation but disabled in E3SM-HR. Neither the E3SM-HR nor the E3SM-LR configurations use a sub-mesoscale eddy transport scheme. The land model is similar to the Community Land Model version 4.5 (Oleson et al. 2013). The Model for Scale Adaptive River Transport (Li et al. 2013, 2015) is used for river routing.

The E3SM-LR simulation is conducted using an atmospheric grid spacing of 110km (1°) and an ocean grid spacing that varies between 30 and 60km. The E3SM-HR simulation uses an atmospheric grid spacing of 28km (0.25°) and an ocean grid spacing that varies between 8 and 16km. These simulations employ transient forcings following the High Resolution Model Intercomparison Project (Haarsma et al. 2016) protocol for the years spanning 1950 through 1969. Both the E3SM-HR and E3SM-LR simulations share the same tuning parameter values − namely, the low-resolution configuration mirrors the "LRtunedHR" simulation described in Caldwell et al. (2019).

TCs were tracked in both data sets using the TempestExtremes software (Ullrich and Zarzycki 2017). The tracking criteria are identical to those recommended by Zarzycki and Ullrich (2017), first identifying candidates as minima in the sea-level pressure field, then culling candidates that do not have an upper-level warm core (defined as a thickness anomaly in the upper-level geopotential). Candidates are then stitched together in time to form trajectories by seeking pairs of candidates at adjacent time levels that are within a specified maximum distance of one another.

3.0   Results

Validation and evaluation are performed against several observational data sets. Observed overland precipitation in the contiguous United States (CONUS) is taken from the Climate Prediction Center (CPC) unified gauge-based analysis precipitation data, a component of the CPC Unified Precipitation Project underway at the National Oceanic and Atmospheric Administration (NOAA) Climate Prediction Center (CPC) covering the period 1948-2014 with a spatial resolution of 0.25° (NOAA Physical Sciences Laboratory 2020). For precipitation outside of the CONUS, the 3-hourly 0.25° gridded 2000-2014 NOAA CPC MORPHing Technique (Joyce et al. 2004, Xie et al. 2017) version 1 data is employed. Our analysis of the biases in the HR model also employs the National Centers for Environmental Prediction (NCEP) atmospheric reanalysis (Kanamitsu et al. 2002) and NOAA sea surface temperatures (Reynolds et al. 2002). Meteorological fields are obtained from the European Centre for Medium-Range Weather Forecasting's ERA5 reanalysis (Hersbach et al. 2020), a retrospective simulation run at 31km horizontal spatial resolution and 1-hourly temporal resolution. Finally, for observational TC tracks, we use the International Best Track Archive for Climate Stewardship (IBTrACS; Knapp et al. 2010), which provides 6-hourly observed TC track data.

We begin our discussion with Figure 1, which already shows striking differences in the quality of two landfalling storms from the E3SM-LR and E3SM-HR simulations. While the E3SM-HR-simulated tropical cyclone includes many well-known TC features, including a well-defined eye, distinct rain bands, and sharp moisture gradients, the E3SM-LR-simulated storm (the only one to make landfall in the CONUS in the 20-year simulation) can be summarized as little more than a large convective blob. With

these striking visual differences in mind, the remainder of this report focuses on the comparative climatology of the E3SM-LR and E3SM-HR simulations.
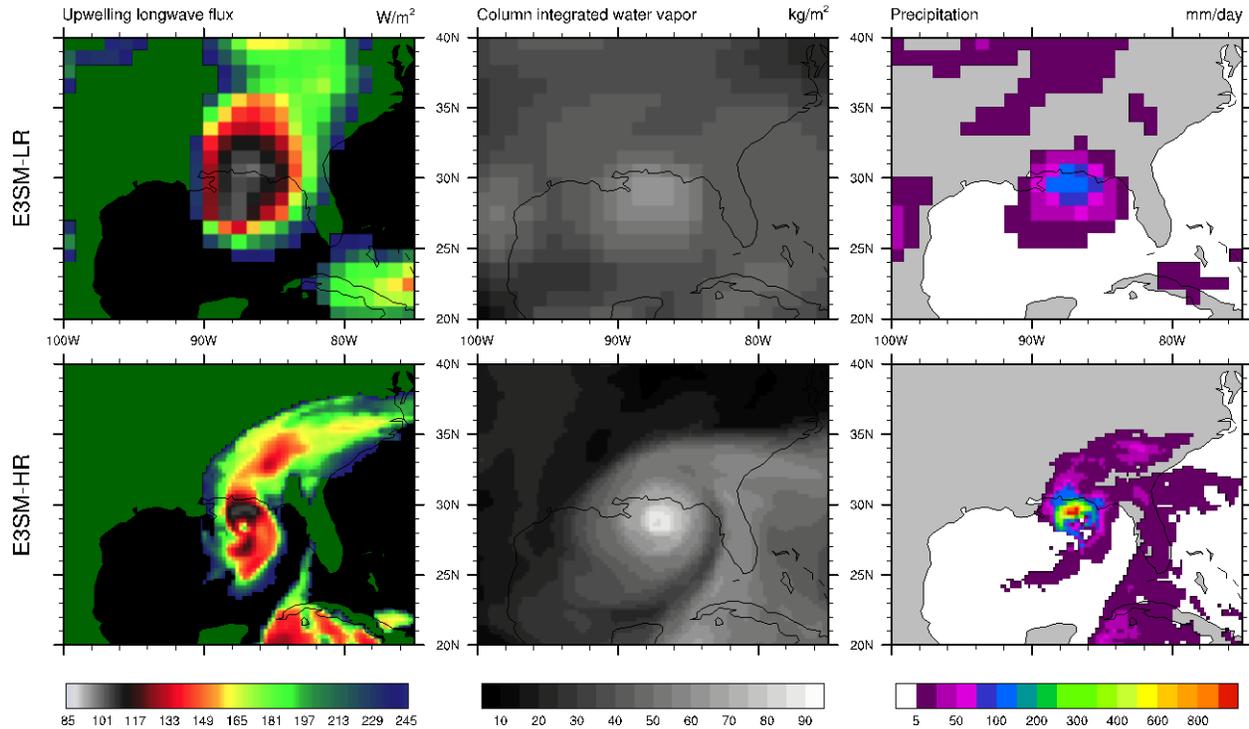
Figure 1. Instantaneous fields showing (left) upwelling longwave flux (i.e., a synthetic infrared satellite image), (middle) column integrated water vapor, and (right) precipitation for two landfalling TCs along the Gulf coast in (top) E3SM-LR and (bottom) E3SM-HR.

3.1 Overall Performance in the North Atlantic

As an initial evaluation of the TC climatology, we compare bulk metrics calculated with the DOE-funded Cyclone Metrics Package (Zarzycki et al. 2021) over the North Atlantic Ocean (NATL). In Figure 2, a Taylor diagram (Taylor 2001) is used for concise evaluation, containing the spatial pattern correlation of NATL TC occurrence (angular distance from vertical axis), total variance (horizontal axis), and annual TC frequency bias (triangular marker). The reference data set is IBTrACS. The closer a point lies to the PERF point (i.e., IBTrACS), the more skillful the model is at simulating NATL TCs. While ERA5 (1) is closest to PERF, this is to be expected as the reanalysis product is highly constrained by observations. Of interest here are the points denoting the mean climatology of the E3SM-HR (2) and E3SM-LR (3) simulations. While the spatial pattern correlation of TC activity is only moderately improved moving from E3SM-LR (0.72) to E3SM-HR (0.79), there are demonstrative improvements in E3SM-HR in both variance and overall TC activity per year. Over the entirety of the NATL, E3SM-HR produces a much more realistic frequency of occurrence and amplitude of storm variations. These improvements with the high-resolution model from a base climatological perspective are key to improving the simulation of landfalling storms that will be discussed in the following sections.
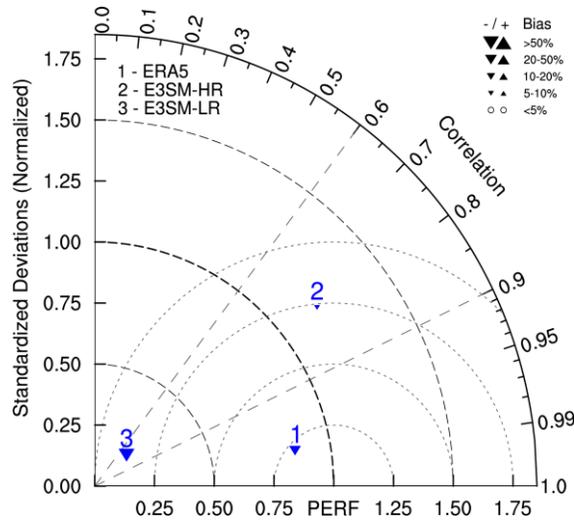
Figure 2. Taylor diagram of aggregated TC statistics. The spatial correlation is plotted as the azimuthal angle while the normalized variance is plotted as the radial distance from the origin. The 'PERF' point represents the observational (IBTrACS) reference. The distance a point lies from the 'PERF' point represents the root mean squared error (dashed concentric isolines). The direction and size of the triangle denotes the TC frequency bias associated with each product.

3.2 Landfalling Storm Count

Given the importance of landfalling TCs to overland precipitation, the decadal frequency of landfalling TCs is shown in Figure 3. The three columns represent the three National Climate Assessment regions (central, southeastern, and northeastern U.S.) that are impacted by TC landfalls. The top row in gray denotes the number of storms per decade that landfall in each of these regions based on observations (1980-2019), while each row below denotes the bias of each data set from the observational reference (e.g., E3SM-HR simulates 2.0 landfalls per decade in the northeastern U.S. [3.8-1.8]).

	CEUS	SEUS	NEUS
IBTrACS	6.8	29.5	3.8
ERA5	-4.2	-11.6	-1.7
E3SM-HR	-3.3	-20.0	-1.8
E3SM-LR	-6.8	-29.0	-3.8

Figure 3. Statistical evaluation of landfalling TCs over the Central U.S. (CEUS), Southeastern U.S. (SEUS), and Northeastern U.S. (NEUS). The top row shows decadal landfalls in IBTrACS over the 1980-2019 period. The next three rows show the landfalling bias in ERA5, E3SM-HR, and E3SM-LR relative to the first line and each cell is shaded based on the magnitude of the bias in each column. Each column represents the three different NCA regions impacted by TCs. Units are number of TC landfalls per decade.

It is clear that the reanalysis and E3SM simulations all underpredict the landfalling frequency of TCs in all three regions (negative biases, blue shading). This is not surprising in light of the general low bias in TC climatology simulated by the HighResMIP models, including even those with fine grid spacing

(Roberts et al. 2020), which is unlikely to be fully mitigated until models push towards 10km grid spacing and below (Davis 2018). However, it is important to note that the low bias seen in E3SM-LR is greatly reduced when moving to the finer grid of E3SM-HR. The improvement in landfalling storms in the Central and Northeastern U.S. regions (e.g., storms such as Harvey and Sandy, respectively) are greatly improved with high resolution. While the improvements are not as great in the Southeastern U.S. (e.g., storms such as Florence, Michael, and Irma), a marked reduction in the low bias is still noted with the E3SM-HR simulation. The low bias in landfalling storms is discussed further in section 3.6 and attributed primarily to a cold bias in sea-surface temperatures (SSTs) in the Gulf of Mexico and along the Atlantic Coast, producing an environment unfavorable for TCs. In fact, the total storm count for the NATL closely matches observations (Figure 2, E3SM-HR triangle), but those storms tend to recurve to the east rather than make landfall in the CONUS.

3.3 Maximum Intensity at Landfall

Storm dynamic intensity (e.g., minimum sea-level pressure) is known to be closely correlated with rainfall intensities and accumulations. Figure 4 shows the locations of landfalls of TCs and their intensity in IBTrACS, ERA5, E3SM-LR, and E3SM-HR. Storm intensity is denoted by the color of the circles at the landfalling locations – all green points are tropical storm strength or weaker, while successively warmer colors denote landfalls of increasing intensity defined by the Saffir-Simpson scale. Since the two E3SM simulations only contain 20 years of data, we have restricted the landfall counts to the post-satellite-period 1980-1999 (inclusive) for IBTrACS and ERA5. When compared to IBTrACS (the top left panel), it is clear that all three gridded data sets underestimate not only landfall frequency (see Figure 3) but also landfall intensity. However, E3SM-HR exhibits significantly improved intensity of landfalling systems, with multiple storms making landfall at Category 1 strength or higher in the simulation – something not seen in the E3SM-LR simulations. Given that ERA5 is constrained by observations, it is also interesting that E3SM-HR remains broadly comparable, underscoring the critical need for the high-resolution grid spacing in order to credibly simulate weather extremes like TCs.
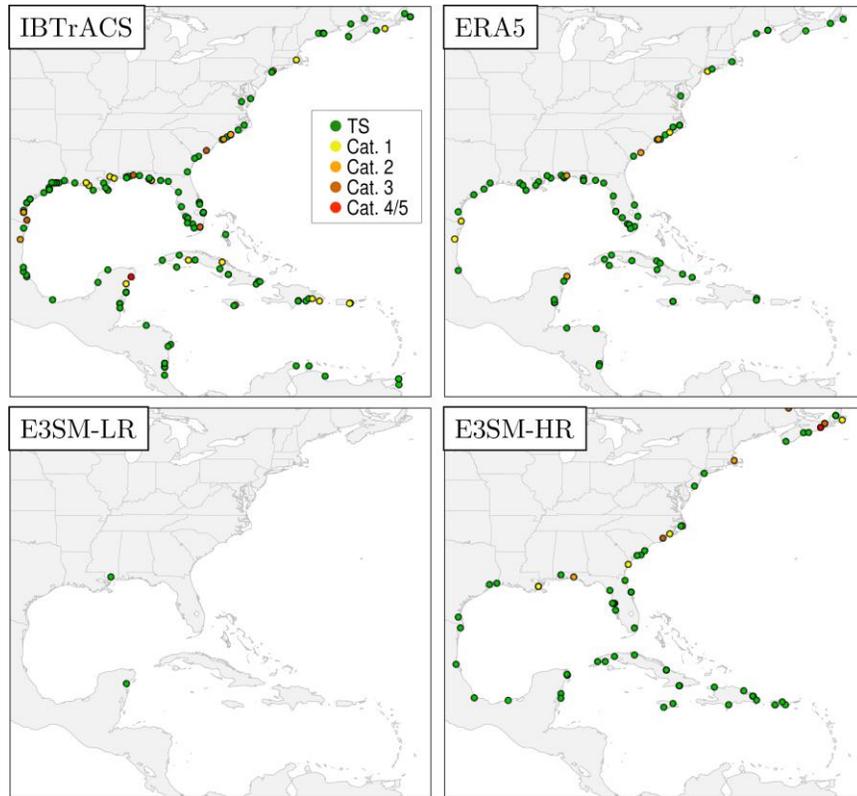
Figure 4. Location and intensity of landfalling TCs in two decades of IBTrACS observations (top left), the ERA5 reanalysis (top right), the E3SM-LR (bottom left), and E3SM-HR (bottom) right. For comparison purposes, the 1980-1999 data is used for the top two panels. Each point denotes a location where a TC intersected a coastal location in the data set, with the color denoting the Saffir-Simpson intensity at landfall as defined by minimum sea-level pressure and the pressure-wind relationship published in Knaff and Zehr (2007).

3.4   Storm Structure

We now analyze the relevant climatological characteristics of individual tropical cyclones, including precipitation structure, surface wind profiles, and storm size.

3.4.1 Precipitation Profiles

As TCs can be approximated in the lowest order as axisymmetric vortices (e.g., Emanuel 1986, Houze Jr. 2010), we focus on radial profiles of azimuthal averages when evaluating TC precipitation and wind profiles. Figure 5a shows the radial profiles of azimuthally averaged precipitation rates for 35-45-knot NATL TCs in the E3SM simulations and comparison to the satellite-based rain rate estimates from CMORPH. Using the NASA TRMM Multi-Satellite Precipitation Analysis (TMPA or TRMM 3B42: Huffman et al. 2007) yields very similar results (not shown).
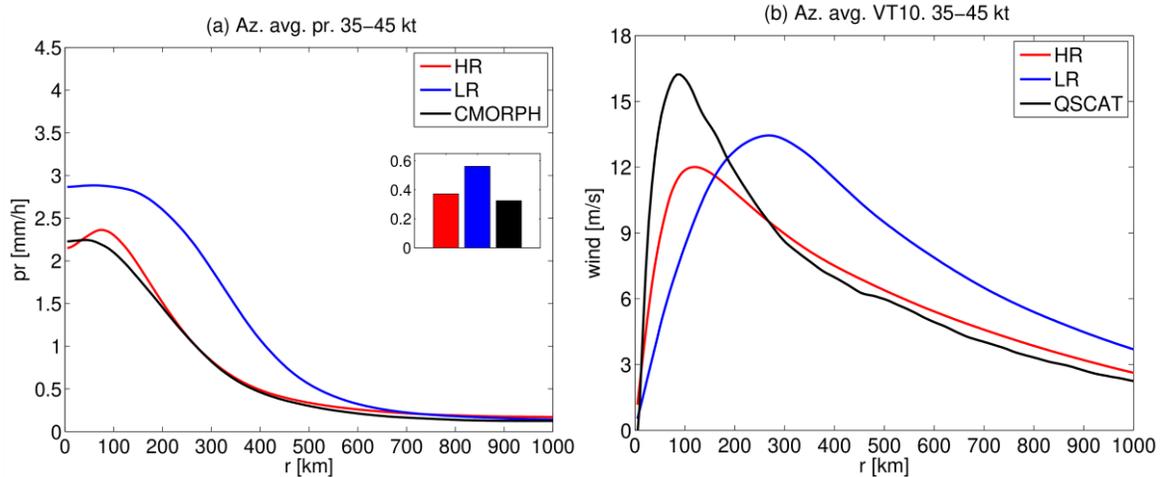
Figure 5. Radial profiles of azimuthally averaged (a) precipitation rates and (b) surface tangential wind for the composites of 35-45-knot TC snapshots in the North Atlantic basin between 0-25°N. The E3SM-HR and E3SM-LR simulations are in red and blue. In (a), the 2000-2014 CMORPH satellite observation is shown in black. In (b), the 2000-2009 QSCAT satellite observation is shown in black. The inset bar graphs in (a) show the area-averaged precipitation rates within $r = 1000$km from the TC center from the above composited radial profiles.

The CMORPH radial profile in Figure 5a (black line) shows TC rainfall decreasing with increasing radius, which is qualitatively reproduced both in the E3SM-HR and E3SM-LR simulations. Quantitatively, the E3SM-LR rainfall structure (blue line) is substantially overestimated in comparison to the CMORPH profile. Using higher horizontal resolution results in significant improvements, as the E3SM-HR (red line) closely resembles the CMORPH profile. The bar graphs in Figure 5a show the area-averaged rain rates within $r = 1000$km from the TC center. While the E3SM-LR simulation produces area-averaged TC rainfall that is substantially (> 70 %) greater than the CMORPH composite, the E3SM-HR simulation is in good agreement with the CMORPH satellite observations.

3.4.2 Wind Profiles

The tangential or azimuthal component of TC wind is the primary TC circulation. Figure 5b compares the radial profiles of azimuthally averaged surface tangential wind for 35-45-knot NATL TCs in the E3SM simulations with the QuikSCAT TC radial structure data set (QSCAT-R: Chavas and Vigh 2014). The radius of the maximum wind (RMW) in the E3SM-LR simulation composite (~ 250km) is significantly greater than the QuikSCAT value (~90km), indicating that TC wind structure is too broad. This is not too surprising given the coarse horizontal resolution (110km) used in the E3SM-LR simulation, which is likely insufficient to fully resolve the mesoscale processes occurring near the TC eyewall. The RMW in the E3SM-HR composite, in contrast, is about 100km, close to that in the QuikSCAT profile. Consistent with the bias in RMW, E3SM-LR substantially underestimates the surface TC tangential wind near the center ($r < 200$km), while overestimating it in the outer regions ($r > 200$km). These biases are much improved in the E3SM-HR simulation (red line), especially in the outer regions. Our results demonstrate that TC rainfall and wind structure in E3SM simulations significantly improves with a higher horizontal resolution.

3.4.3 Storm Size

Azimuthal wind speed is also valuable for estimating NATL TC storm size (Stansfield et al. 2020). Here $r8$ is employed to quantify the storm size, defined as the outermost radius of winds exceeding 8 m/s. This is a common measure of the size of the outer circulation of TCs and is important for determining the size of the precipitation field. Figure 6 shows the normalized distributions of $r8$ for the E3SM simulations and the ERA5 data set for 1985-2014, for all TCs at all times in their lifetimes. As in Figure 5b, the E3SM-LR simulation tends to overestimate $r8$, because the TCs are under-resolved at the low resolution. The E3SM-HR simulation has an $r8$ distribution more consistent with ERA5, although the median (marker on the x axis) is larger than the ERA5 distribution median by about 150km. While all NATL TCs are included in this analysis, this level of agreement is consistent with analogous results for storms that have completed landfall (not shown).
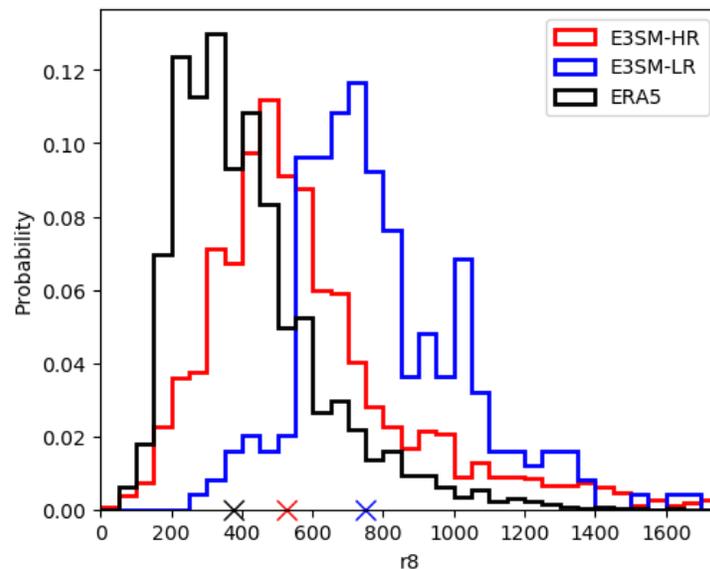
Figure 6. Normalized distributions of $r8$ (km) in 50km bins for E3SM-HR, E3SM-LR, and ERA5 for all NATL TCs at all times in their lifetimes. The X markers on the x axis mark the medians of the distributions.

3.5 Landfalling Precipitation Accumulations

Precipitation from TCs over the Eastern U.S. between the E3SM-HR and E3SM-LR simulations is now assessed in comparison to a combination of observations and reanalysis. Here precipitation is taken from the daily CPC analysis, and TC tracks are obtained from application of our TC tracking procedure to ERA5 (due to data availability, only years 1985-2014 are used). The combination of these data sets and the methodology was used to compare TC precipitation over the Eastern U.S. in several variable-resolution Community Atmosphere Model (CAM) configurations in Stansfield et al. (2020). TC tracks from ERA5 are used instead of an observational data set to allow a fairer comparison for the models and to keep the TC tracking methodology consistent between the models and observations. ERA5 also provides the meteorological fields needed to estimate the outer size (i.e., radius of 8 m/s winds) as the TC precipitation extraction radius for observed storms.

We focus primarily on extreme precipitation from TCs, which we quantify with the Rx5day index, defined as the annual maximum 5-day accumulated precipitation. The left column of Figure 7 shows the annual mean Rx5day over the Eastern U.S. Although E3SM underestimates Rx5day overall, the E3SM-HR simulation indeed outperforms E3SM-LR in the Southeastern U.S. Looking at the annual mean Rx5day attributed to TCs in the middle column, the E3SM simulated precipitation is still low compared to observations, but E3SM-HR dramatically outperforms E3SM-LR. The right column of Figure 7 shows the annual mean percentage of Rx5day events that are due to TCs. Although some regions attribute more than 30% of Rx5day events to TCs in observations, the largest values from the E3SM-HR simulation are 20-25%, as found in the Southeastern U.S. Nonetheless, E3SM-HR further demonstrates its superiority over E3SM-LR in this metric, since the E3SM-LR simulation shows practically no Rx5day events are caused by TCs. In fact, the E3SM-HR simulation biases can be almost exclusively attributed to the low bias in landfalling storms pointed out in section 3.2 (as opposed to the structure of individual storms). To clearly demonstrate this claim, normalized TC Rx5day for E3SM-HR is calculated by multiplying TC Rx5day by the number of landfalling storms in ERA5 divided by the number of landfalling storms in E3SM-HR (fourth row of Figure 7), producing a map which closely matches the observed results in the top row of Figure 7. These results clearly suggest that if biases in landfalling storm frequency were improved, total overland extreme precipitation from TCs is also likely to show commensurate improvement.

3.6 Sources for Model Bias in E3SM-HR Simulations

Although the E3SM-HR simulations show dramatic improvement in the quality of simulated tropical cyclones over the E3SM-LR simulation, we expect that further improvements could be realized through directed model improvements. We now discuss some potential sources of bias in the large-scale TC environment that, if mitigated, could greatly improve the climatology of landfalling storms.

In the tropical North Atlantic, the model bias in TC genesis resembles a zonal dipole with predominantly negative biases in the western Atlantic to the west of 60°W, and positive biases to its east in the eastern Atlantic (Figure **Error! Reference source not found.**a). Further to the north, there is also a region of positive bias in TC genesis to the west of 40°W. These biases in model TC genesis can mostly be explained by those in the simulated thermodynamic environment. Positive biases in Potential Intensity (PI; Emanuel 1986, Holland 1997) are found in the eastern tropical Atlantic and in the northwest Atlantic along the U.S. east coast (Figure **Error! Reference source not found.**b). In these regions, the large-scale thermodynamic environment is more favorable for TC formation and development. On the other hand, in the western Atlantic we have negative biases in PI, especially in the Caribbean Sea and the Gulf of Mexico. In these regions, the environment is less conducive for TCs, consistent with the overall negative biases in TC genesis.
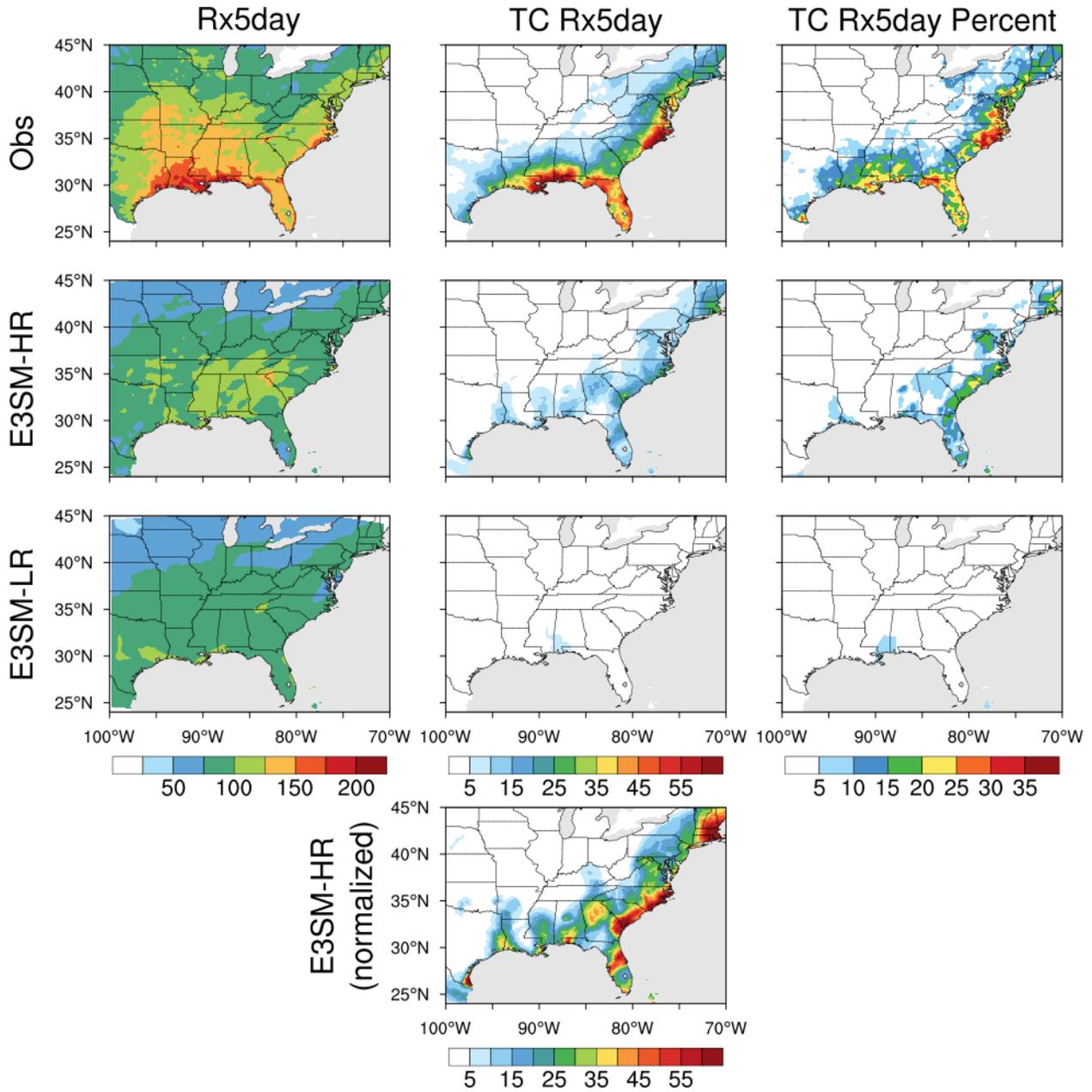
Figure 7. (Left column) Annual mean Rx5day (mm/year), (middle column) annual mean Rx5day from TCs (mm/year), and (right column) annual mean percentage of Rx5day events that are due to TCs (%) for (first row) observations, (second row) E3SM-HR simulation, and (third row) E3SM-LR simulation. The fourth row shows the E3SM-HR TC Rx5day normalized by the number of landfalling TCs.
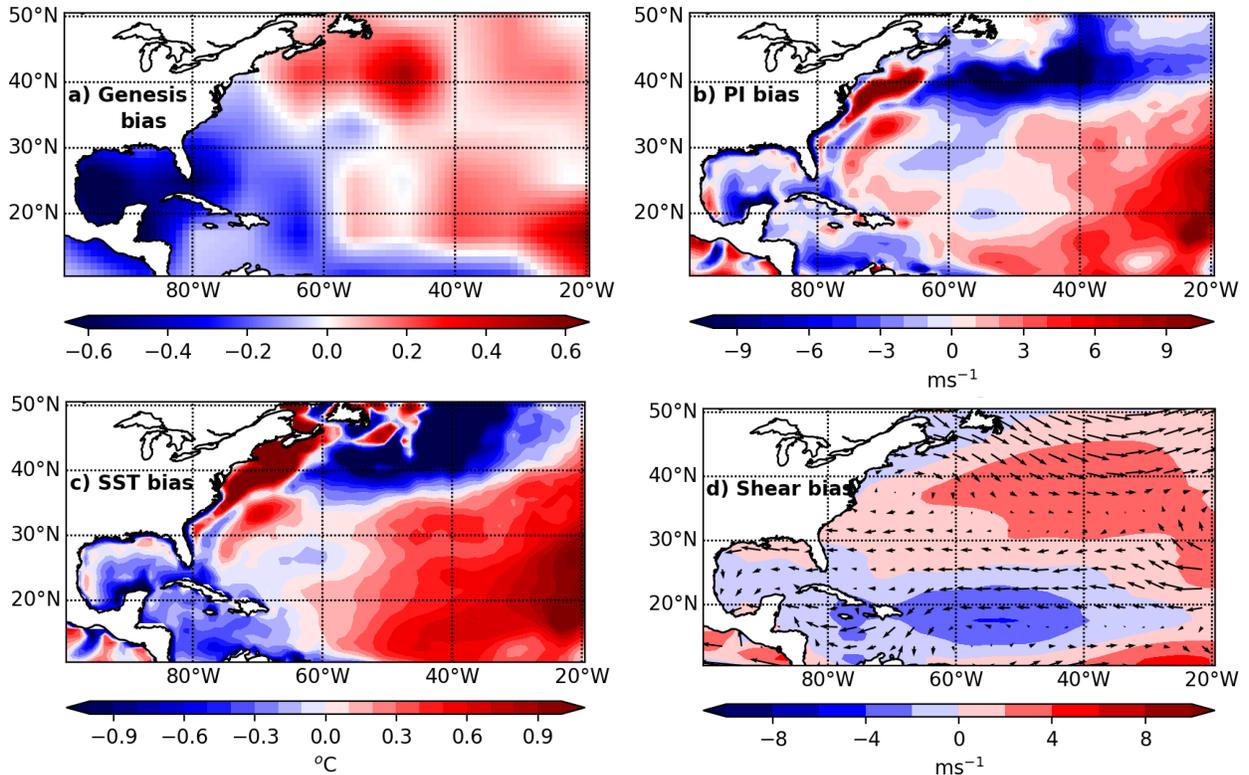
Figure 8. E3SM-HR bias in (a) TC genesis, (b) Potential Intensity (ms^{-1}), (c) SST (^{o}C), and (d) Vertical wind shear (ms^{-1}). The vectors in panel D represent errors in steering flow. The various parameters in panels B, C, and D are averaged over the Atlantic TC season (June-November). The observational analysis is based on NCEP atmospheric reanalysis and NOAA SSTs.

An examination of model SST biases (Figure 8c) reveals that biases in PI can mostly be explained by those in SSTs. Climatologically, TCs tend to intensify in the western Atlantic where warm SSTs traditionally reside. Thus, the negative SST and PI biases in these regions likely play a role in the weaker-intensity TCs produced by the model. Besides TC genesis and intensity, biases in the thermodynamic environment can also play a role in the simulated TC tracks. The positive biases in PI occur in regions where TCs have a greater tendency to recurve (Kossin et al. 2010). Similarly, the negative PI biases in the western tropical Atlantic suppress the formation of those TCs that have a higher chance of landfall and a smaller tendency to recurve. The overall effect of this is to produce a relatively larger fraction of TCs in the model that tend to recurve and avoid landfall in the U.S.

Besides thermodynamic biases, the simulated large-scale dynamic environment can also drive biases in TC landfall. Biases in vertical wind shear are negative in much of the TC main development region (Figure 8d). Thus, to the east of 60˚W the dynamic environment promotes TC development in tandem with the thermodynamic environment. However, in the western Atlantic, the dynamic environment is unable to overcome the negative impacts of SST biases. In the extra-tropics, there are positive biases in shear suggesting that the dynamic environment, along with the thermodynamic environment, is less favorable for TCs, especially to the east of 60˚W. Finally, we consider biases in steering flow to understand the impact of errors in simulation of large-scale winds on TC landfall (Figure 8d). In the region to the east of the Caribbean islands, the anomalous steering flow is southward, which tends to push

TCs to the south and reduce U.S. landfall. Even in the Gulf of Mexico, to the south of 25˚N, the anomalous steering flow has a southward component. Thus, model biases in steering flow, in combination with the unfavorable thermodynamic environment in the western Atlantic, tend to decrease TC landfall in the Gulf of Mexico.

3.7 Summary

Significant improvements have been identified in E3SM-HR relative to E3SM-LR in many TC metrics including TC occurrence, the radial profiles of azimuthally averaged precipitation rates and surface tangential winds, and TC storm sizes in the North Atlantic. Importantly, landfalling TC metrics including the number of landfalling TCs and extreme precipitation from landfalling TCs also show considerable improvements in E3SM-HR compared to E3SM-LR. Despite the significant positive impact of model resolution on modeling TC frequency and characteristics, biases in the large-scale environment of the atmosphere and ocean have limited the number of TCs making landfall on the eastern and Gulf coasts. This motivates the need for improving the large-scale climatology of the coupled model to support modeling of TC coastal impact. Further improvements in landfalling storm intensity may also be realized with even finer grid spacing and improved sub-grid representation of turbulence and precipitation.

Many of the evaluation capabilities showcased in this report are available as open-source software packages that comply with the Coordinated Model Evaluation Capabilities (CMEC) standards for model evaluation tools. The DOE-funded CMEC standards provide a development framework for community-oriented developers, and enable robust and consistent evaluation of general climate data sets with a variety of metrics and diagnostics.

4.0   References

Balaguru, K, LR Leung, LP Van Roekel, JC Golaz, PA Ullrich, PM Caldwell, SM Hagos, BE Harrop, and A Mametjanov. 2020. "Characterizing Tropical Cyclones in the Energy Exascale Earth System Model Version 1." *Journal of Advances in Modeling Earth Systems* 12(8): e2019MS002024, https://doi.org/10.1029/2019MS002024

Caldwell, PM, A Mametjanov, Q Tang, LP Van Roekel, J-C Golaz, W Lin, DC Bader, ND Keen, Y Feng, R Jacob, ME Maltrud, AF Roberts, MA Taylor, M Veneziani, H Wang, JD Wolfe, K Balaguru, P Cameron-Smith, L Dong, SA Klein, LR Leung, H-Y Li, Q Li, X Liu, RB Neale, M Pinheiro, Y Qian, PA Ullrich, S Xie, Y Yang, Y Zhang, K Zhang, and T Zhou. 2019. "The DOE E3SM coupled model version 1: Description and results at high resolution." *Journal of Advances in Modeling Earth Systems* 11(12): 4095−4146, https://doi.org/10.1029/2019MS001870

Chavas, DR, and J Vigh. 2014. QSCAT-R: The QuikSCAT tropical cyclone radial structure dataset. Technical report. NCAR Technical Note TN-5131STR.

Davis, CA. 2018. "Resolving tropical cyclone intensity in models." *Geophysical Research Letters* 45(4): 2082–2087, https://doi.org/10.1002/2017GL076966

Dennis, JM, J Edwards, KJ Evans, O Guba, PH Lauritzen, AA Mirin, A St-Cyr, MA Taylor, and PH Worley. 2012. "CAM-SE: A scalable spectral element dynamical core for the Community Atmosphere Model." *International Journal of High Performance Computing Applications* 26(1): 74–89, https://doi.org/10.1177/1094342011428142

Emanuel, KA. 1986. "An air-sea interaction theory for tropical cyclones. Part I: Steady-state maintenance." *Journal of the Atmospheric Sciences* 43(6): 585–605, https://doi.org/10.1175/1520-0469(1986)043<0585:AASITF>2.0.CO;2

Gent, PR, and JC McWilliams. 1990. "Isopycnal mixing in ocean circulation models." *Journal of Physical Oceanography* 20(1): 150−155, https://doi.org/10.1175/1520-0485(1990)020<0150:IMIOCM>2.0.CO;2

Gettelman, A, and H Morrison. 2015. "Advanced two-moment bulk microphysics for global models. Part I: Off-line tests and comparison with other schemes." *Journal of Climate* 28(3): 1268–1287, https://doi.org/10.1175/JCLI-D-14-00102.1

Gettelman, A, H Morrison, S Santos, P Bogenschutz, and PM Caldwell. 2015. "Advanced two-moment bulk microphysics for global models. Part II: Global model solutions and aerosol-cloud interactions." *Journal of Climate* 28(3): 1288–1307, https://doi.org/10.1175/JCLI-D-14-00103.1

Golaz, JC, VE Larson, and WR Cotton. 2002. "A PDF-Based Model for Boundary Layer Clouds. Part I: Method and Model Description." *Journal of the Atmospheric Sciences* 59(24): 3540–3551, https://doi.org/10.1175/1520-0469(2002)059<3540:APBMFB>2.0.CO;2

Haarsma, RJ, MJ Roberts, PL Vidale, A Catherine, A Bellucci, Q Bao, P Chang, S Corti, NS Fučkar, V Guemas, J Von Hardenberg, W Hazeleger, C Kodama, T Koenigk, LR Leung, J Lu, JJ Luo, J Mao, MS Mizielinski, R Mizuta, P Nobre, M Satoh, E Scoccimarro, T Semmler, J Small, and JS Von Storch. 2016. "High Resolution Model Intercomparison Project (HighResMIP v1.0) for CMIP6." *Geoscientific Model Development* 9(11): 4185–4208, https://doi.org/10.5194/gmd-9-4185-2016

Hersbach, H, B Bell, P Berrisford, S Hirahara, A Horányi, J Muñoz-Sabater, J Nicolas, C Peubey, R Radu, D Schepers, A Simmons, C Soci, S Abdalla, X Abellan, G Balsamo, P Bechtold, G Biavati, J Bidlot, M Bonavita, G De Chiara, P Dahlgren, D Dee, M Diamantakis, R Dragani, J Flemming, R Forbes, M Fuentes, A Geer, L Haimberger, S Healy, RJ Hogan, E Holm, M Janiskova, S Keeley, P Laloyaux, P Lopez, C Lupu, G Radnoti, P de Rosnay, I Rozum, F Vamborg, S Villaume, and J-N Thepaut. 2020. "The ERA5 global reanalysis." *Quarterly Journal of the Royal Meteorological Society* 146(730): 1999–2049, https://doi.org/10.1002/qj.3803

Holland, GJ. 1997. "The maximum potential intensity of tropical cyclones." *Journal of the Atmospheric Sciences* 54(21): 2519–2541, https://doi.org/10.1175/1520-0469(1997)054<2519:TMPIOT>2.0.CO;2

Houze Jr., RA. 2010. "Clouds in tropical cyclones". *Monthly Weather Review* 138(2): 293–344, https://doi.org/10.1175/2009MWR2989.1

Huffman, GJ, DT Bolvin, EJ Nelkin, DB Wolff, RF Adler, G Gu, Y Hong, KP Bowman, and EF Stocker. 2007. "The TRMM Multisatellite Precipitation Analysis (TMPA): Quasi-global, multiyear, combined-sensor precipitation estimates at fine scales." *Journal of Hydrometeorology* 8(1): 38–55, https://doi.org/10.1175/JHM560.1

Iacono, MJ, JS Delamere, EJ Mlawer, MW Shephard, SA Clough, and WD Collins. 2008. "Radiative forcing by long-lived greenhouse gases: Calculations with the AER radiative transfer models." *Journal of Geophysical Research – Atmospheres* 113(D13): D13103, https://doi.org/10.1029/2008JD009944

Joyce, RJ, JE Janowiak, PA Arkin, and P Xie. 2004. "CMORPH: A method that produces global precipitation estimates from passive microwave and infrared data at high spatial and temporal resolution." *Journal of Hydrometeorology* 5(3): 487–503, https://doi.org/10.1175/1525-7541(2004)005<0487:CAMTPG>2.0.CO;2

Kanamitsu, M, W Ebisuzaki, J Woollen, SK Yang, J Hnilo, M Fiorino, and G Potter. 2002. "NCEP–DOE AMIP-II Reanalysis (r-2)." *Bulletin of the American Meteorological Society* 83(11): 1631–1644, https://doi.org/10.1175/BAMS-83-11-1631

Knaff, JA, and RM Zehr. 2007. "Reexamination of tropical cyclone wind–pressure relationships." *Weather and Forecasting* 22(1): 71–88, https://doi.org/10.1175/WAF965.1

Knapp, KR, MC Kruk, DH Levinson, HJ Diamond, and CJ Neumann. 2010. "The international best track archive for climate stewardship (IBTrACS) unifying tropical cyclone data." *Bulletin of the American Meteorological Society* 91(3): 363–376, https://doi.org/10.1175/2009BAMS2755.1

Kossin, JP, SJ Camargo, and M Sitkowski. 2010. "Climate modulation of North Atlantic hurricane tracks." *Journal of Climate* 23(11): 3057–3076, https://doi.org/10.1175/2010JCLI3497.1

Larson, VE. 2017. CLUBB-SILHS: A parameterization of subgrid variability in the atmosphere. arXiv 1711.03675.

Larson, VE, and JC Golaz. 2005. "Using probability density functions to derive consistent closure relationships among higher-order moments." *Monthly Weather Review* 133(4): 1023–1042, https://doi.org/10.1175/MWR2902.1

Leung, LR, DC Bader, MA Taylor, and RB McCoy. 2020. "An introduction to the E3SM special collection: Goals, science drivers, development, and analysis." *Journal of Advances in Modeling Earth Systems* 12(11): e2019MS001821, https://doi.org/10.1029/2019MS001821

Li, H, MS Wigmosta, H Wu, M Huang, Y Ke, AM Coleman, and LR Leung. 2013. "A physically based runoff routing model for land surface and earth system models." *Journal of Hydrometeorology* 14(3): 808–828, https://doi.org/10.1175/JHM-D-12-015.1

Li, HY, LR Leung, A Getirana, M Huang, H Wu, Y Xu, J Guo, and N Voisin. 2015. "Evaluating global streamflow simulations by a physically based routing model coupled with the community land model." *Journal of Hydrometeorology* 16(2): 948–971, https://doi.org/10.1175/JHM-D-14-0079.1

Liu, X, PL Ma, H Wang, S Tilmes, B Singh, RC Easter, SJ Ghan, and PJ Rasch. 2016. "Description and evaluation of a new four-mode version of the Modal Aerosol Module (MAM4) within version 5.3 of the Community Atmosphere Model." *Geoscientific Model Development* 9(2): 505–522, https://doi.org/10.5194/gmd-9-505-2016

Mlawer, EJ, SJ Taubman, PD Brown, MJ Iacono, and SA Clough. 1997. "Radiative transfer for inhomogeneous atmospheres: RRTM, a validated correlated-k model for the longwave." *Journal of Geophysical Research – Atmospheres* 102(D14): 16 663–16 682, https://doi.org/10.1029/97JD00237

NOAA Physical Sciences Laboratory. 2020. CPC Unified Gauge-Based Analysis of Daily Precipitation over CONUS. https://psl.noaa.gov/data/gridded/data.unified.daily.conus.html

Oleson, KW, DM Lawrence, GB Bonan, B Drewniak, M Huang, CD Koven, S Levis, F Li, WJ Riley, ZM Subin, SC Swenson, PE Thornton, A Bozbiyik, R Fisher, CL Heald, E Kluzek, JF Lamarque, PJ Lawrence, LR Leung, W Lipscomb, S Muszala, DM Ricciuto, W Sacks, Y Sun, J Tang, and ZL Yang. 2013. Technical description of version 4.5 of the Community Land Model (CLM). NCAR/TN-478+STR NCAR Technical Note : 26610.5065/D6RR1W7M.

Petersen, MR, XS Asay-Davis, AS Berres, Q Chen, N Feige, MJ Hoffman, DW Jacobsen, PW Jones, ME Maltrud, SF Price, TD Ringler, GJ Streletz, AK Turner, VLP Van Roekel, M Veneziani, JD Wolfe, PJ Wolfram, and JL Woodring. 2019. "An Evaluation of the Ocean and Sea Ice Climate of E3SM Using MPAS and Interannual CORE-II Forcing." *Journal of Advances in Modeling Earth Systems* 11(5):1438–1458, https://doi.org/10.1029/2018MS001373

Pielke Jr., RA, J Gratz, CW Landsea, D Collins, MA Saunders, and R Musulin. 2008. "Normalized hurricane damage in the United States: 1900–2005." *Natural Hazards Review* 9(1): 29–42, https://doi.org/10.1061/(ASCE)1527-6988(2008)9:1(29)

Rasch, PJ, S Xie, P-L Ma, W Lin, H Wang, Q Tang, SM Burroughs, P Caldwell, K Zhang, RC Easter, P Cameron-Smith, B Singh, H Wan, J-C Golaz, BE Harrop, E Roesler, J Bacmeister, VE Larson, KJ Evans, Y Qian, M Taylor, LR Leung, Y Zhang, L Brent, M Branstetter, C Hannay, S Mahajan, A Mametjanov, R Neale, JH Richter, J-H Yoon, CS Zender, D Bader, M Flanner, JG Foucar, R Jacob, N Keen, SA Klein, X Liu, AG Salinger, M Shrivastava, and Y Yang. 2019. "An overview of the Atmospheric Component of the Energy Exascale Earth System Model." *Journal of Advances in Modeling Earth Systems* 11(8): 2377−2411, https://doi.org/10.1029/2019MS001629

Reynolds, RW, NA Rayner, TM Smith, DC Stokes, and W Wang. 2002. "An improved in situ and satellite SST analysis for climate." *Journal of Climate* 15(13): 1609–1625, https://doi.org/10.1175/1520-0442(2002)015<1609:AIISAS>2.0.CO;2

Richter, JH, and PJ Rasch. 2008. "Effects of convective momentum transport on the atmospheric circulation in the Community Atmosphere Model, version 3." *Journal of Climate* 21(7): 1487–1499, https://doi.org/10.1175/2007JCLI1789.1

Ringler, T, M Petersen, RL Higdon, D Jacobsen, PW Jones, and M Maltrud. 2013. "A multi-resolution approach to global ocean modeling." *Ocean Modelling* 69: 211–232, https://doi.org/10.1016/j.ocemod.2013.04.010

Roberts, MJ, J Camp, J Seddon, PL Vidale, K Hodges, B Vanniere, J Mecking, R Haarsma, A Bellucci, E Scoccimarro, LP Caron, F Chauvin, L Terray, S Valcke, MP Moine, D Putrasahan, C Roberts, R Senan, C Zarzycki, and P Ullrich. 2020. "Impact of model resolution on tropical cyclone simulation using the HighResMIP-PRIMAVERA multimodel ensemble." *Journal of Climate* 33(7): 2557–2583, https://doi.org/10.1175/JCLI-D-19-0639.1

Stansfield, AM, KA Reed, CM Zarzycki, PA Ullrich, and DR Chavas. 2020. "Assessing tropical cyclones' contribution to precipitation over the Eastern United States and sensitivity to the variable-resolution domain extent." *Journal of Hydrometeorology* 21(7): 1425–1445, https://doi.org/10.1175/JHM-D-19-0240.1

Taylor, KE. 2001. "Summarizing multiple aspects of model performance in a single diagram." *Journal of Geophysical Research: Atmospheres* 106(D7): 7183–7192, https://doi.org/10.1029/2000JD900719

Ullrich, PA, and CM Zarzycki. 2017. "TempestExtremes: A framework for scale-insensitive pointwise feature tracking on unstructured grids." *Geoscientific Model Development* 10(3): 1069–1090, https://doi.org/10.5194/gmd-10-1069-2017

Xie, P, R Joyce, S Wu, SH Yoo, Y Yarosh, F Sun, and R Lin. 2017. "Reprocessed, bias-corrected CMORPH global high-resolution precipitation estimates from 1998." *Journal of Hydrometeorology* 18(6): 1617–1641, https://doi.org/10.1175/JHM-D-16-0168.1

Zarzycki, CM, PA Ullrich, and KA Reed. 2021. "Metrics for evaluating tropical cyclones in climate data." *Journal of Applied Meteorology and Climatology* https://doi.org/10.1175/JAMC-D-20-0149.1

Zarzycki, CM, and PA Ullrich. 2017. "Assessing sensitivities in algorithmic detection of tropical cyclones in climate data." *Geophysical Research Letters* 44(2): 1141–1149, https://doi.org/10.1002/2016GL071606

Zhang, GJ, and NA McFarlane. 1995. "Sensitivity of climate simulations to the parameterization of cumulus convection in the Canadian climate centre general circulation model." *Atmosphere-Ocean* 33(3): 407−446, https://doi.org/10.1080/07055900.1995.9649539